Effect of Material Variability on Multiscale Modeling of Rate-Dependent Composite Materials

Joel Johnston[1] and Aditi Chattopadhyay[2]

Abstract: The effects of material variability on the mechanical response and failure of composites under high strain rate and impact loading are investigated in this paper. A previously developed strain rate–dependent, sectional micromechanics model is extended to account for the variability in microstructure and constituent material properties. The model presented in this paper also includes a three-dimensional damage law based on a work potential theory and a microscale failure criterion. Microstructural characterization of the composite is performed to obtain the statistical distributions needed for the stochastic methodologies. A Latin hypercube sampling technique is used to model the uncertainties in fiber volume fraction and viscoplastic material constants. A comparison of general Monte Carlo simulation and Latin hypercube–based Monte Carlo shows that the Latin hypercube technique converges using fewer simulations. The modulus and failure strain obtained using the developed methodology show good correlation with the experimental data. This novel stochastic sectional model is shown to correlate better with the available experimental data compared with the deterministic sectional model. A laminate level, parametric study is also conducted to investigate the effect of uncertainty on the residual energy of a composite laminate during impact. **DOI: 10.1061/(ASCE)AS.1943-5525.0000488.**

Author keywords: Multiscale model; Stochastic; Variability; Polymer matrix composite; Latin hypercube; Micromechanics.

Introduction

Polymer matrix composite (PMC) materials are increasingly being used in airframe and engine applications. However, damage initiation and failure mechanisms in composites are still not fully understood and are an ongoing area of research. A multiscale modeling framework with scale-dependent constitutive laws and an appropriate failure theory is required to capture the behavior and failure of composite structures subjected to complex loadings. In applications to engine containment systems, such as a fan blade separating from the rotor during operation, the system's ability to prevent impact failure is an important factor. The rate dependency and nonlinearity of PMC materials further increases the complexity of the models required to simulate an impact event. In addition, variability in the material constituents plays an important role. The systematic consideration of uncertainties is as important as having the appropriate structural model, especially during model validation where the total error between physical observation and model prediction must be characterized. It is necessary to quantify the effects of uncertainties at every length scale in order to fully understand their impact on the structural response. Material variability may include variation in fiber volume fraction (V_f), fiber diameter, fiber waviness, and void distributions. Therefore, a stochastic modeling framework with scale-dependent constitutive laws and an appropriate failure theory is required to simulate the behavior and failure of PMC structures subjected to complex loadings. The model must have the ability to account for uncertainties, strain rate effects, and transverse shear stresses to capture the entirety of an impact event. The objective of this paper is to develop an efficient numerical framework for the analysis of PMC structures addressing several of these issues.

A key component to modeling composite behavior in impact applications is capturing the essential rate-dependent behavior through viscoplastic theories. Sun and Chen (1989) developed a single-parameter plasticity model consisting of a quadratic yield function, associated flow rule, and plastic potential to capture the nonlinear behavior of composites. A characterization study was performed by Tsai and Sun (2002) to determine the optimal specimen geometry for the state variables of a single-parameter plasticity model with strain rate effects. Experimentation and modeling of co-woven-knitted composites was performed by Sun et al. (2014) using a simplified geometric model of the microstructure and a flow potential plasticity law. Thiruppukuzhi and Sun (2001) developed a two- and three-parameter overstress viscoplastic theory with a rate-dependent failure criterion. The strain rate–dependent behavior of composites has also been modeled using a quadratic stress function in an overstress viscoplastic theory (Gates and Sun 1991), a constant rate power and three-dimensional viscoplastic law (Weeks and Sun 1998), and an overstress viscoplastic model that included multiaxial effects (Eisenberg and Yen 1981).

A significant amount of work has been reported on simulating the behavior and failure mechanisms of composite materials for high strain rate and impact applications using deterministic approaches. Yen (2002) incorporated a delamination failure criterion using a continuum damage mechanics (CDM) framework and integrated the model within the nonlinear finite-element software *LS-DYNA* (Hallquist 2007). Souza et al. (2008) developed a multiscale model incorporating viscoelasticity in a micromechanical model and a cohesive zone model to determine the effect of damage under impact loadings. Voyiadjis et al. (2001) developed a multiscale model including damage and plasticity variables at the mesoscale and macroscale. Yu and Fish (2002) used asymptotic homogenization for the spatial and temporal domains to model viscoelastic behavior of composites. Hettich et al. (2008) created a variational model that decomposed the displacement field to model

[1]Graduate Research Associate, Arizona State Univ., 551 East Tyler Mall, Tempe, AZ 85287 (corresponding author). E-mail: Joel.Johnston@asu.edu

[2]Regents' Professor, Arizona State Univ., 551 East Tyler Mall, Tempe, AZ 85287.

Note. This manuscript was submitted on August 1, 2014; approved on January 12, 2015; published online on February 17, 2015. Discussion period open until July 17, 2015; separate discussions must be submitted for individual papers. This paper is part of the ***Journal of Aerospace Engineering***, © ASCE, ISSN 0893-1321/04015003(9)/$25.00.

cracks at different length scales. Macroscopic failure of composite structures was modeled using a multiscale progressive failure technique by Laurin et al. (2007). Pineda et al. (2009) and Pineda (2012) used an integrated work potential damage theory within a generalized method of cells model to simulate the progression of microscale damage in composites. Tabiei et al. (2005) performed impact simulations of composites through a combination micromechanical model integrated in *LS-DYNA* that captured the rate-dependent behavior and laminate level failure.

Various micromechanical models have been developed to simulate the nonlinear behavior and properties of PMCs. The method of cells (MOC) was developed by Aboudi (1989) for unidirectional fiber-reinforced composites with elastoviscoplastic constituents. The MOC was further developed into a generalized method of cells (GMC) by Paley and Aboudi (1992) for unidirectional composites. Pindera and Bednarcyk (1999) reformulated the GMC using simplified uniform stress and strain assumptions, resulting in improved computational efficiency. By applying a similar approach to the MOC and discretizing the composite unit cell into three subcells, a two-dimensional elastic-plastic model was developed by Sun and Chen (1991). This model was then extended to three dimensions by Robertson and Mall (1993). A more precise elastic micromechanics model was proposed by Whitney (1993) in which the unit cell was divided into an arbitrary number of rectangular, horizontal slices. Mital et al. (1995) used a slicing approach to compute the effective elastic constants and microstresses (fiber and matrix stresses) in ceramic matrix composites. In their work, a mechanics of materials approach was used to compute the effective elastic constants and microstresses in each slice of a unit cell. Laminate theory was then applied to obtain the effective elastic constants for the unit cell as well as the effective stresses in each slice. The slicing approach was extended to include the material nonlinearity and strain rate dependency in the deformation analysis of PMCs, and used to investigate the impact response of thin laminated plates subjected to in-plane loading (Goldberg et al. 2004, 2005; Goldberg 2000, 2001). The slice micromechanical model was modified to incorporate out-of-plane, transverse shear effects to simulate the transient and impact responses of composite shells (Zhu et al. 2005, 2006b; Zhu 2006). The slice model was further extended to a three-dimensional sectional micromechanics model (Zhu 2006; Zhu et al. 2008, 2006a). The sectional micromechanics model applied a decoupling concept to the fiber-matrix unit cell that was able to capture the full three-dimensional stress and strain components as well as the transverse isotropy of the material. Liu (2011) and Liu et al. (2011) used a numerical micromechanics model based on GMC to study the rate-dependent behavior and failure of composites with complex architecture. In their work, small fiber undulations were allowed and the homogenization process was decomposed to introduce normal and shear coupling. Yekani Fard et al. (2011a, b, 2012b, a) characterized the effect of the stress gradient in flexure on constitutive laws for polymeric materials and revised the uniaxial tension and compression strength to simulate the flexural strength for any strain rate.

Developing methodologies that can identify and quantify the parametric variability is crucial. Liu and Ghoshal (2014) demonstrated criteria capable of quantifying and reconstructing the microstructural variability of composite materials. Naito et al. (2008) characterized the constituent properties of several types of carbon fiber and defined statistical distributions for the properties. For stochastic multiscale models, it is important to consider the propagation of microstructural variability to larger length scales as well as the constituent property and geometric variability at the larger length scales. Ghosh et al. (2001) developed a multiscale Voronoi cell finite-element approach using random microstructure to analyze composite failure. Chamis (2004) presented a stochastic multiscale framework that used fast probability integration to incorporate uncertainty in the material properties.

The objective of this study is to develop a multiscale approach to model the response and failure of PMC materials including variability and strain rate dependency. The sectional micromechanics theory, previously developed by Zhu et al. (2008, 2006a), is extended to include the effects of material variability and microscale damage. Microstructural characterization was performed to determine the statistical distribution of the fiber volume fraction. A viscoplastic constituent law is used to simulate rate-dependent and impact behavior of PMC materials. The molecular flow parameter, rate-dependence parameter, and Young's modulus of the polymeric resin are also used as random variables by assuming normal distributions. Details of the stochastic methodology and micromechanics can be found in the following sections. The Hashin failure criteria and damage theory for the macroscale was integrated in the original sectional micromechanics. A microscale, work potential damage theory and microscale failure criterion are incorporated in the current stochastic sectional micromechanics model. The multiscale methodology, comprising the sectional micromechanics and progressive failure theory, is used within a commercial finite-element analysis package, *LS-DYNA*, to study the effect of material variability on the impact behavior of PMC laminates. The random variables used in the impact simulations are the initial projectile velocity and the fiber volume fraction. Case studies of various model responses for unidirectional IM7/977-2 composite material are presented in the results section.

Variability Analysis

Microstructural Characterization

Characterization of the composite was performed to obtain the statistical distributions for the stochastic methodologies. Image quantification was performed on the PMC material using optical microscopy (Zeiss LSM 700) to obtain the variability in the fiber volume fraction (V_f). Fig. 1(a) shows a small portion of the microstructure for a PMC laminate as well as the random location of the fibers within the resin. A binary filtering was applied to the images obtained from the microscopy in order to differentiate between the fiber and the polymer matrix. The boxed area in Fig. 1(a) represents an area where a V_f value can be computed. Similar areas were defined at various locations of the micrograph and used to compute the V_f distribution. A convergence study was performed to determine the appropriate size of the boxed areas and number of boxed areas to be extracted from a single image. From this convergence study, it was determined that 20,000 boxed areas were required to accurately capture the V_f distribution and the converged dimensions of the boxed areas was 300 by 300 μm. The Bayesian information criterion (BIC) is used to determine the optimal distribution type for each data set (Schwarz 1978). The BIC performs model selection similar to the likelihood function but also contains a penalty term to avoid overfitting Eq. (1)

$$\mathrm{BIC} = -2 \ln L(\hat{\theta}_k | y) + k \ln n \tag{1}$$

In Eq. (1), L is the likelihood function where $\hat{\theta}_k$ represents the parameter values that maximize the likelihood function and y represents the observed data points. The variables k and n denote the number of free parameters and the number of data points contained in y, respectively. In order to determine the best-fit distribution, continuous distributions such as the normal, extreme value, t location scale, Weibull, and logistic distributions were fitted to the data

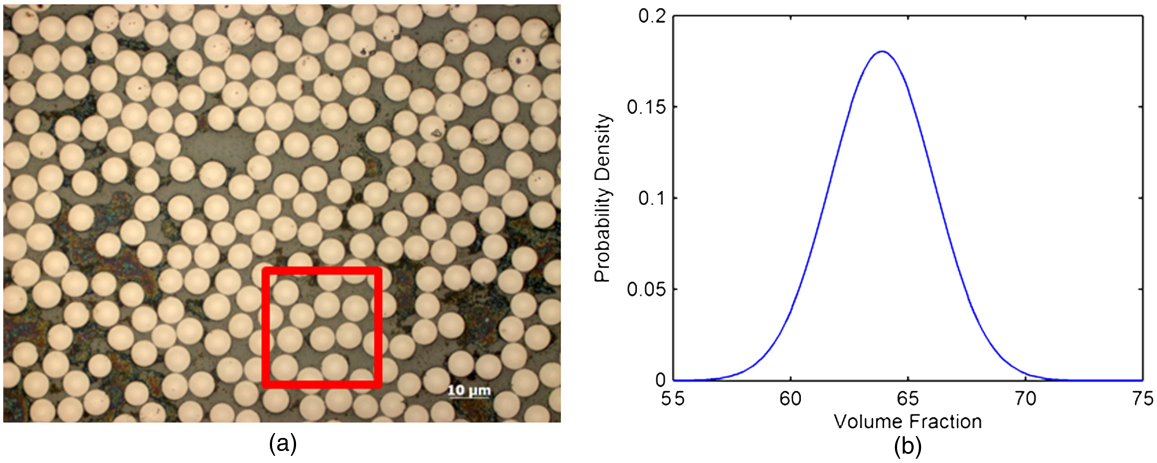

Fig. 1. (a) PMC microstructure; (b) PMC probability density function of V_f

using these criteria. In the previously mentioned convergence study, the best-fit distribution varied as the number of boxed areas and size of boxed areas changed. Using the converged values, a normal distribution was found to be the best fit and the probability density function is shown in Fig. 1(b). The average and standard deviation parameters for the normal distribution are 63.9 and 2.21%, respectively. A nominal V_f value of 67.5% was calculated from the image, which is similar to the average value from the normal distribution. Deterministic composite models use the average V_f to determine a periodic structure of the composite using a unit cell of a single fiber in resin.

Stochastic Techniques

Two different stochastic methodologies were investigated in this paper. The Latin hypercube sampling (LHS) technique uses an approach similar to stratified sampling within a Monte Carlo methodology. The LHS sampling discretizes the cumulative distribution function given by a random input and it randomly assigns a point within each discretized interval. By performing LHS sampling, the distribution function can be defined with fewer samples compared to completely random sampling. The number of samples required for a stochastic modeling technique is an important factor because it is equivalent to the number of simulations necessary within the sectional micromechanics model.

The probability density function of V_f from Fig. 1(b) was considered as a random variable and used as an input to the sectional micromechanics model by introducing a stochastic methodology. The best-fit distribution of the V_f correlated to a normal probability density function described by Eq. (2) and the cumulative distribution function (CDF) was calculated using the function in Eq. (3)

$$f(x) = \frac{1}{\sigma\sqrt{2\pi}} e^{-[(x-\mu)^2/(2\sigma^2)]} \tag{2}$$

$$F(x) = \frac{1}{2}\left[1 + \text{erf}\left(\frac{x-\mu}{\sqrt{2\sigma^2}}\right)\right] \tag{3}$$

where x = manifested value of fiber volume fraction. The mean and standard deviation of the V_f are shown as μ and σ, respectively. These cumulative distributions are continuous functions operating on a range of values from 0 to 1. This range is discretized using LHS through a set number of simulations, N. Examples of the random and LHS methods (using 20 simulations) are shown in Fig. 2, where one simulation represents a single value of V_f. The random sampling of the fiber volume fraction CDF is sparse on the right portion of the plot, while the LHS represents the entire distribution well and randomness is still captured within the discretized intervals. The points computed within these intervals represent CDF values and Eq. (3) can be inverted to calculate a V_f point.

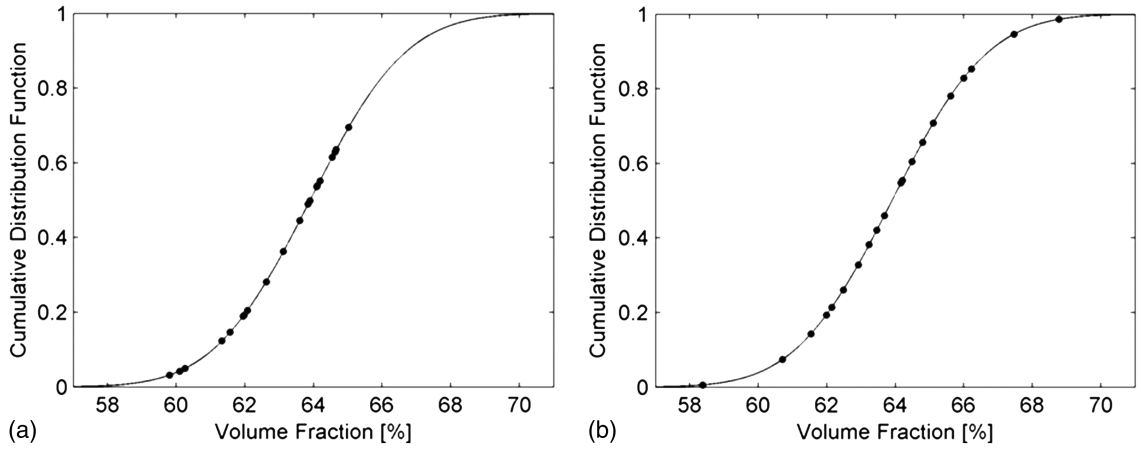

Fig. 2. (a) Cumulative distribution functions of V_f with random sampling Monte Carlo; (b) cumulative distribution functions of V_f with LHS Monte Carlo

Index #	V_f	Z	. . .	*ith variable*
1				X
2		X		
3				
4	X			
.				
.				
.				
N				

Input Variables for First Run: V_f(4), Z(2), …

Fig. 3. Latin hypercube selection process

As depicted in Fig. 3, each representation of the V_f is entered into a table. For multiple random parameters, a single representation of the V_f is randomly paired with the other parameter and arranged into parameter sets. The set of parameters was used as inputs for the stochastic sectional micromechanics (SSM) model.

Multiscale Modeling

Stochastic Sectional Micromechanics

The sectional micromechanical model developed by Zhu (2006) and Zhu et al. (2006a, 2008) used an MOC-type approach and accounts for three-dimensional parameters of the material including in-plane deformation, transverse shear deformation, and through the thickness normal deformation. The discretization process of the sectional micromechanics is illustrated in Fig. 4, which assumes that the repeating unit cell of the composite is a single fiber in a matrix. Due to the symmetry only a quarter of the unit cell is analyzed and, through sectioning, the system of equations of the unit cell is decoupled into three systems of equations. Two of the systems of equations are from section A and section B and the third system of equations is the system of equations of the unit cell. The model assumes the composite material has square fiber packing and a perfect interfacial bond between the fiber and matrix. The relations between the subcells and sections assume stress and strain continuity conditions, and the boundaries of the unit cell are assumed to be periodic. The stress and strain increments of the subcells are assumed to be uniform, and the stress and strain increments of the unit cell are obtained from volume-averaging techniques. Details of the continuity relations between subcells and sections are provided by Zhu (2006). This sectional micromechanics model was further extended by introducing material parameter variability at the microscale using the LHS technique discussed in the previous section. The parameter sets that were defined using the stochastic methodology were assigned to the respective constituent subcells. The outcome of the SSM theory was the full three-dimensional stress and strain behavior of the material accounting for material variability.

The constitutive equations for the fiber subcells are represented by a transversely isotropic, linear elastic model Eq. (4), whereas the polymer subcells are represented by a modified Bodner-Partom viscoplastic state variable model (Bodner 2002). Rate dependency and inelasticity is incorporated in the viscoplastic model, which is of particular interest for capturing the progressive damage behavior of the composite laminate under impact loading. The modification of the viscoplastic model consisted of an additional hydrostatic stress term and the details are given by Goldberg et al. (2005) and expressed in Eqs. (5) and (6). This viscoplastic model was incorporated within the constitutive law for the polymer subcells Eq. (7)

$$d\varepsilon_i^f = S_{ij}^f d\sigma_j^f \qquad i,j = 1,\ldots,6 \tag{4}$$

$$\dot{\varepsilon}_{ij}^I = 2D_0 \exp\left[-\frac{1}{2}\left(\frac{Z}{\sigma_e}\right)^{2n}\right]\left(\frac{\sigma_{ij}^{\text{dev}}}{2\sqrt{J_2}} + \alpha\delta_{ij}\right) \tag{5}$$

$$\sigma_e = \sqrt{3J_2} + \sqrt{3}\alpha\sigma_{kk} \tag{6}$$

$$d\varepsilon_i^m = S_{ij}^m d\sigma_j^m + d\varepsilon_i^I \qquad i,j = 1,\ldots,6 \tag{7}$$

In Eq. (4), the variables $d\varepsilon^f$ and $d\sigma^f$ represent the strain and stress increments of the fiber subcells, respectively, and S^f contains the components of the compliance matrix for the fiber subcells. In Eqs. (5)–(7), Z and α are variables related to the resistance of molecular flow and hydrostatic stress effects, respectively, D_0 is the maximum inelastic strain rate, and the variable n controls the rate dependence of the material. The variable σ^{dev} contains the deviatoric stress components, J_2 is the second invariant of the deviatoric stress tensor, and σ_{kk} is the summation of normal stress components. The variables $d\varepsilon^m$ and $d\sigma^m$ represent the strain and stress increments of the polymer matrix subcells, respectively, and S^m contains the components of the compliance matrix for the polymer matrix subcells. The variable de^I is the inelastic strain increment of the polymer matrix subcells, which is obtained from Eq. (5).

In addition to material variability, the SSM model also incorporates a microscale damage progression theory and a microscale failure criterion. The microscale damage progression theory introduced is based on a work potential model (Schapery 1990), which is a thermodynamics-based model that is able to capture microscale damage by discretizing the strain energy into elastic and damage components. The work potential theory was further used in a plane stress damage theory developed by Pineda et al. (2009) and Pineda (2012), where it was integrated with a GMC approach. The microscale, progressive damage theory used in the current SSM model

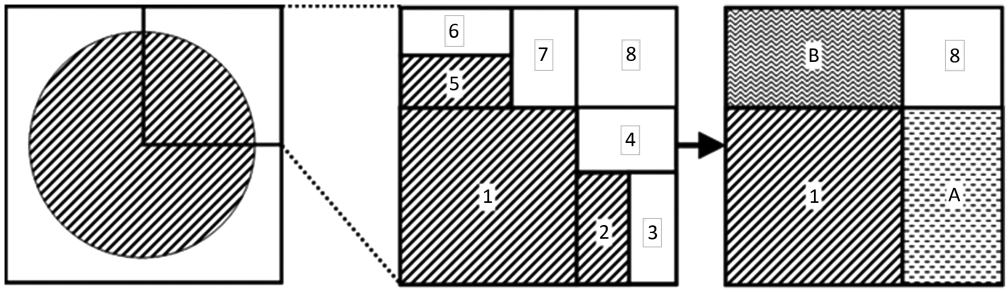

Fig. 4. Discretization process of unit cell in sectional micromechanics (data from Zhu 2006b)

was applied to the matrix subcells and uses an incremental, three-dimensional derivation of the strain energy density described by Eq. (8)

$$U^{k+1} = U^k + \frac{1}{2} d\varepsilon_{ij}(2\sigma_{ij}^{k+1} - d\sigma_{ij}) \tag{8}$$

$$d\sigma_{ij} = \sigma_{ij}^{k+1} - \sigma_{ij}^{k} \tag{9}$$

$$U = W + S \tag{10}$$

$$S_r = S^{1/3} \tag{11}$$

In Eqs. (8) and (10), U represents the total three-dimensional strain energy density, the superscript k denotes the increment index, and $d\sigma_{ij}$ is the incremental stress. After the total strain energy density for an increment is calculated, it can be expressed as the sum of the elastic strain energy density, W, and the strain energy density associated with damage and structural changes, S [Eq. (10)]. Due to experimental convenience, the reduced damage parameter, S_r, was introduced to replace the original damage variable, S, and this relationship is shown in Eq. (11). A matrix damage curve (Fig. 5) was calculated from the experimental work reported by Gilat et al. (2002) in which a hydraulic Instron frame was used to conduct the tensile testing of polymeric specimens. A damage value of 1 represents the undamaged state and a damage value of 0 is the fully damaged state. The procedure for determining a damage curve is outlined in the work reported by Sicking (1992). The microscale failure criterion was also applied to the matrix subcells where the stress in the each subcell was set to zero when the stress for each subcell exceeded the failure strength of the polymer. The macroscale failure criterion was based on a modified Hashin failure theory (Zhu et al. 2008; Hashin 1980) that incorporates the shear stress effect in the compressive fiber failure mode, which was not considered in the original Hashin failure theory. Eqs. (12) and (13) describe the failure criteria for the fiber subcells in tension and compression, respectively. Eqs. (14) and (15) describe the failure criteria for the polymer matrix subcells in tension and compression, respectively. The four failure modes are formulated as functions of the failure strengths of the composite material. The parameters σ_A^+ and σ_A^- represent the tensile and compressive failure strengths in the fiber direction, respectively. The parameters σ_T^+ and σ_T^- represent the tensile and compressive failure strengths perpendicular to the fiber direction, respectively. The parameters τ_T and τ_A represent the transverse and axial shear strengths, respectively.

$$\left(\frac{\sigma_{11}}{\sigma_A^+}\right)^2 + \frac{1}{\tau_A^2}(\sigma_{12}^2 + \sigma_{13}^2) = 1 \qquad \sigma_{11} > 0 \tag{12}$$

$$\left(\frac{\sigma_{11}}{\sigma_A^-}\right)^2 + \frac{1}{\tau_A^2}(\sigma_{12}^2 + \sigma_{13}^2) = 1 \qquad \sigma_{11} < 0 \tag{13}$$

$$\frac{1}{(\sigma_T^+)^2}(\sigma_{22} + \sigma_{33})^2 + \frac{1}{\tau_T^2}(\sigma_{23}^2 - \sigma_{22}\sigma_{33}) + \frac{1}{\tau_A^2}(\sigma_{12}^2 + \sigma_{13}^2) = 1$$
$$\sigma_{22} + \sigma_{33} > 0 \tag{14}$$

$$\frac{1}{\sigma_T^-}\left[\left(\frac{\sigma_T^-}{2\tau_T}\right)^2 - 1\right](\sigma_{22} + \sigma_{33}) + \frac{1}{4\tau_T^2}(\sigma_{22} + \sigma_{33})^2 + \frac{1}{\tau_T^2}(\sigma_{23}^2 - \sigma_{22}\sigma_{33}) + \frac{1}{\tau_A^2}(\sigma_{12}^2 + \sigma_{13}^2) = 1$$
$$\sigma_{22} + \sigma_{33} < 0 \tag{15}$$

Impact Simulation

A multiscale model consisting of the sectional micromechanics and Hashin failure theory was integrated in a user-defined material subroutine within the *LS-DYNA* nonlinear finite-element software to simulate the impact behavior of a PMC laminate under various loading conditions. A parametric study was performed to determine the variability in laminate impact simulations. The V_f and initial velocity were the designated parameters for the study. The laminated circular plate was 200 mm in diameter and comprised four IM7/977-2 unidirectional laminae with a $[0_4]$ stacking sequence and lamina thickness of 0.5 mm. A fixed boundary condition was applied to the nodes on the circumference of the composite laminate. The steel projectile measured 40 mm in diameter and 80 mm in length and was modeled as an elastic material. The plate and projectile were meshed using brick elements with a single integration point per element for improved computational efficiency. Mesh refinement was implemented in the central region of the composite plate near the impact location due to the presence of large stress and strain gradients caused by the high strain rate impact event. The meshed composite plate and projectile geometries are presented in Fig. 6. The number of elements used in the model was 6,496 elements for the composite laminate and 320 elements for the steel projectile. The dynamic simulations were executed with explicit time integration using adaptive time steps. An eroding contact card was defined in *LS-DYNA* and coupled with the failure model to accurately account for the elements that were no longer able to

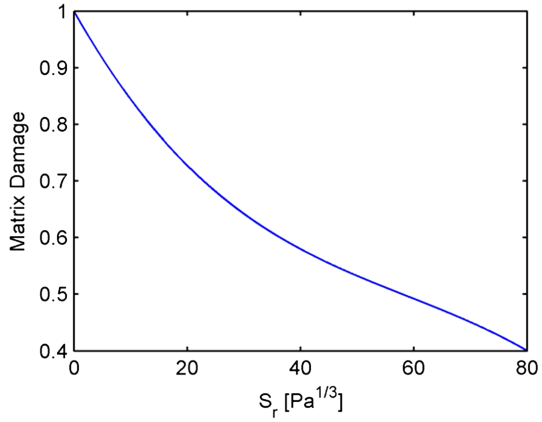

Fig. 5. Matrix damage curve from experimental data

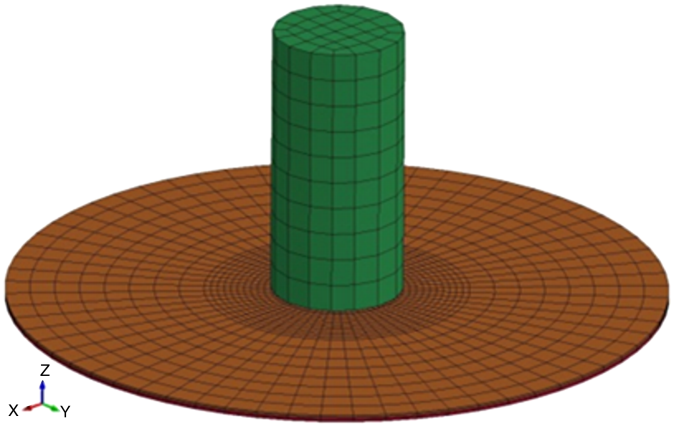

Fig. 6. Meshed geometries for impact simulation

carry load. The element erosion was determined by the previously described failure criterion. When an element failed it was deleted and the contact surfaces were automatically updated.

Results

Case I: Sampling Method Comparison

A comparison of general Monte Carlo simulation (MCS) and LHS-based Monte Carlo was conducted to investigate the accuracy and efficiency of each method. The statistical distribution parameters for the V_f were calculated using the previously mentioned variability analysis and the parameter statistics are provided in Table 1. The coefficient of variation (COV) is a normalized measure used to calculate the dispersion of a probability distribution. The transverse failure strength and failure strain were considered, and the resulting COV values are shown in Fig. 7. Both general MCS and LHS-based Monte Carlo are displayed in these plots. A key distinction in Fig. 7 is that the converged value for the transverse strength COV is approximately 0.28%, while the COV for the transverse strain is 1.95%. Therefore the transverse failure strain exhibits a larger dispersion of the variability compared with the transverse failure strength due to the assumed random variables. Analysis shows that while both methods converge at approximately the same COV value, the LHS converged in a fewer number of simulations. The COV value was assumed to have already converged by a simulation count of 1,000 and convergence was indicated when the difference in COV values was consistently within 3%. Specifically, LHS required 80% fewer simulations for convergence when comparing the COV trend of the failure stress plot, and 95% fewer simulations for convergence when comparing the COV trend of the failure strain plot.

Case II: Stochastic Micromechanics Results with Multiple Random Variables

It is shown in the first case that the LHS approach was the more efficient of the two sampling methods. Therefore the LHS approach was used, with a simulation count of 100, for all Case II results. This simulation count was shown in Case I to accurately represent the variability. However, it is important to note that this count was based on a single random variable and further analysis is necessary to determine the appropriate simulation count for multiple random variables. The results in Case II were obtained by modeling the transverse tension loading of the material under a strain rate of 1 s^{-1}. The V_f, elastic modulus of the resin, and several variables from the viscoplastic model Eq. (3) were speculated to affect the variability in the transverse, tensile response, therefore they were chosen as random variables in Case II. The distribution and parameters for V_f were experimentally determined as previously discussed. However, normal distributions were assumed for the remaining random variables in Table 1 and the statistics for these distributions are presented in the table. These assumed values were used to study the effect of variability using the SSM model; more realistic distributions should be determined experimentally.

Comparisons of the SSM model were made with tensile experimental data (Gilat et al. 2002) using a strain rate of approximately 1 s^{-1} on a hydraulic Instron frame. Different combinations of the damage and failure theories are depicted in Fig. 8(a) to demonstrate the benefit of the additional theories. The comparisons were made with the deterministic analysis to better illustrate the impact of the different damage theories. The figure shows that the transverse response obtained using the integrated damage theory, comprising microscale damage, microscale failure, and macroscale failure, has close correlation with experiments. For the figure legends and tabulated results, Macro refers to the model with only the modified Hashin criteria applied, Damage/Macro refers to the model with the microscale work potential theory as well as the modified Hashin criteria, and Damage/Micro/Macro indicates the combination of the microscale damage and failure criteria as well as the modified Hashin theory. Fig. 8(b) compares the stochastic response obtained using the previously mentioned integrated damage theory with the experimental results. Statistical results were extracted for the failure strain, failure strength, and modulus because these three parameters represent the behavior and failure of the material. Error analysis was performed on the statistical results and the results are presented in Tables 2 and 3 as average and minimum percent difference values using the experimental data as a reference. Table 2 presents a comparison of the stochastic sectional model using only the Hashin failure criteria from the original sectional micromechanics model previously developed in Zhu et al. (2006b). There is a minimal decrease in the average error values of the statistical parameters as multiple random variables are introduced, but a large

Table 1. Random Variable Statistics

Parameters	V_f (%)	Z (Pa)	n	E_m (Pa)
Standard deviation	2.21	1.08×10^7	0.0325	0.09×10^8
Average	63.90	2.59×10^8	0.8515	3.52×10^9

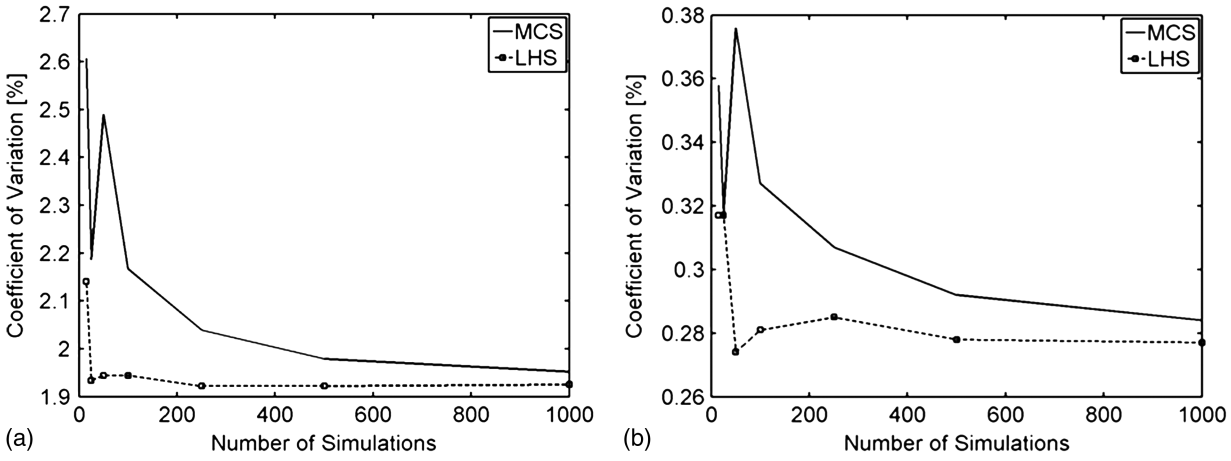

Fig. 7. Comparison of COV with a varying number of simulations of MCS and LHS using transverse failure (a) strain and (b) strength

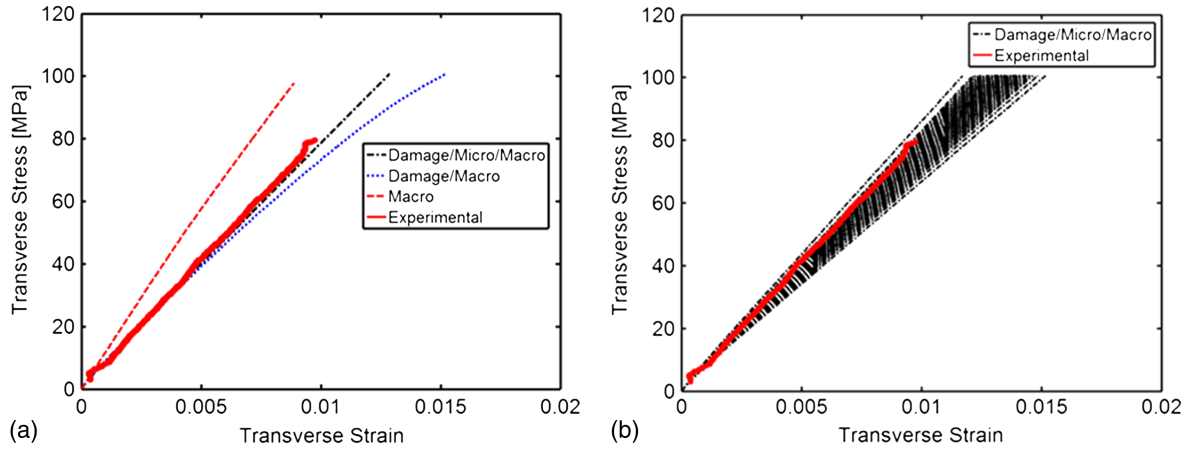

Fig. 8. (a) Comparison of experimental data (Gilat et al. 2002) and transverse model responses with different failure and damage theories for low strain rate loading; (b) comparison of stochastic transverse response with experimental results

Table 2. Experimental Comparison of Multiple Random Variables

Parameters	Random variables (%)				Deterministic
	V_f	V_f and Z	V_f, Z, and n	V_f, Z, n, and E_m	
Minimum difference in failure strain	11.14	10.81	2.89	2.89	18.15
Average difference in failure strain	17.30	17.31	17.06	17.06	18.15
COV of failure strain	1.99	2.00	2.74	3.01	0
Minimum difference in failure strength	12.36	12.27	12.22	12.25	13.18
Average difference in failure strength	12.97	12.96	12.96	12.95	13.18
COV of failure strength	0.26	0.28	0.28	0.27	0
Minimum difference in modulus	25.41	24.71	19.79	19.81	29.46
Average difference in modulus	28.90	28.83	28.58	28.55	29.46
COV of modulus	1.78	1.89	2.40	2.62	0

Table 3. Experimental Comparison of Failure and Damage Theories

Parameters	Macro (%)	Damage/ macro (%)	Damage/ micro/ macro (%)
Minimum difference in failure strain	2.89	18.58	7.29
Average difference in failure strain	17.06	33.73	20.13
Minimum difference in failure strength	12.25	15.60	15.53
Average difference in failure strength	12.95	15.67	15.65
Minimum difference in modulus	19.81	0.54	~0
Average difference in modulus	28.55	12.11	8.06

decrease in the minimum error is observed for failure strain and modulus as multiple random variables are added. Because the experimental data consist of a single curve, the minimum error value is a better error measure for stochastic results because it represents the possibility of one of the stochastic curves being the same as the experimental curve. The average error value represents a trend of the data and would be a more appropriate error measure for a statistically relevant number of experimental specimens. The entries in Table 3 are statistical results from different combinations of the damage and failure theories using all four random parameters. A small increase in minimum error is observed for failure strain and failure strength, but there is a significant decrease in the minimum error for the modulus. The stochastic micromechanics results should be compared to a statistically relevant set of experimental data to fully validate the statistical results.

Case III: Impact Simulations of a PMC Laminate

Parametric studies were conducted to analyze the failure behavior and residual velocity of the composite plate by varying the V_f and initial projectile velocity. For each parameter, simulations were performed using the same boundary conditions and were processed using time durations that allowed the projectile to penetrate through the composite plate. Stress, strain, and displacement field variables were output for all simulations as well as the velocity of the projectile at every time step. The tabulated velocity data were plotted and used to compute the residual velocity of the projectile. The velocity of the projectile played a noticeable role in the damage behavior of the impacted composite plate. During an impact event, a portion of the kinetic energy of the projectile was transferred to the composite plate. Therefore, variation of the initial projectile velocity altered the degree and rate of energy transfer. The simulated damage progression is presented in Fig. 9 for a projectile traveling at 250 m/s and impacting the laminate. The geometry was sectioned along a vertical plane to provide a better view of the impact behavior near the projectile–plate interface. As the projectile contacted the plate, the elements on the top surface failed under out-of-plane shear, crushing (compression), and fragmentation. Analysis of the projectile velocity before and after the impact event provides an estimate of the energy absorption of the composite plate under impact.

Fig. 10 shows the ballistic limits of composite laminates as a function of fiber volume fraction; the ballistic limit increases as the V_f increases. The ballistic limit is defined as the velocity required

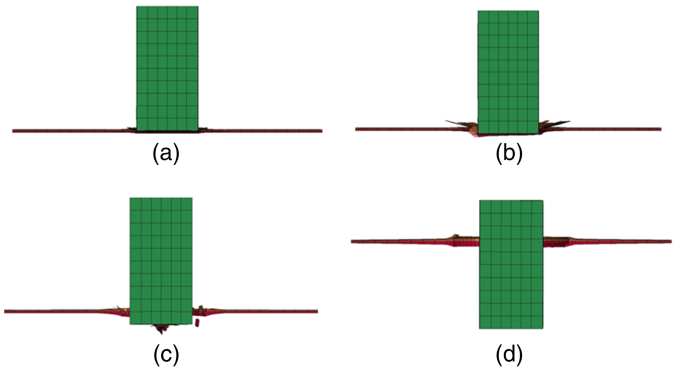

Fig. 9. Progression of projectile through a composite laminate with an initial velocity of 250 m/s: (a) projectile impact; (b) shear, crushing, or fragmentation failure of laminae; (c) projectile punching through laminate; (d) projectile penetrating through laminate

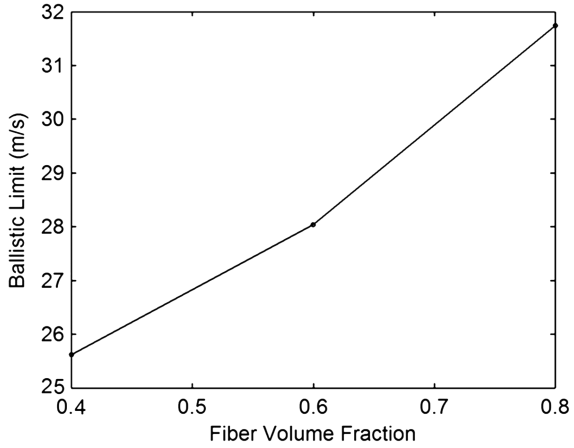

Fig. 10. Ballistic limit of composite laminates with varying fiber volume fractions

for a projectile to fully penetrate a material specimen and is shown in Eq. (16) (Jenq et al. 1994). The parameter v_p represents the velocity of the projectile immediately before impact and v_r is the residual velocity of the projectile after impact

$$v_{\mathrm{BL}} = \sqrt{v_p^2 - v_r^2} \tag{16}$$

Because the density of the fibers is greater than that of the matrix, a larger V_f increases the overall density of the composite. Therefore a greater amount of energy was absorbed by the denser composite laminates. In addition, because the fiber can sustain higher stresses before failure, the composite remained intact for a longer period of time during the impact event, thereby providing more time for the plate to absorb energy from the high speed projectile. A larger number of laminae would absorb more energy, which would cause a greater increase in the ballistic limit.

Concluding Remarks

The SSM model was used to demonstrate the effect of material variability on the composite response due to high strain rate loading. Several cases were studied to verify the stochastic methodology and to examine the mechanical behavior and failure of the composite material at different length scales. For Case I, the COV measure was calculated to determine the number of simulations needed to reach a converged level of variation. The Case I analysis showed that a simulation count of 100 was sufficient to capture the variability when using the LHS method, whereas a higher simulation number is needed for MCS. In Case II, the effect of variability was investigated on the failure strain, failure strength, and modulus of the transverse response. When compared with experimental data, the SSM results in Case II revealed that the incorporation of variability, microscale damage, and microscale failure theories enabled the model to capture the behavior and failure with 7% error in failure strain and approximately zero error in modulus. These errors indicated a better correlation was achieved by using the current SSM model compared with the deterministic sectional model, which showed an 18% error in failure strain and 29% error in modulus. Ideally the stochastic micromechanics results should be compared with a statistically relevant set of experimental data to fully validate the model. However, due to a limitation in the available and experimental data, especially at higher strain rates, the simulation results were compared with small experimental data sets. The results presented show that the available experimental data are within the range of the stochastic micromechanics results and further testing is necessary to determine its robustness over a wider range of parameter variability. The multiscale model was used within *LS-DYNA* to simulate the high velocity impact of a PMC laminate using an elastic projectile and the results were presented in Case III. The result of the impact simulations demonstrated that the ballistic limit increased when the V_f was increased.

Acknowledgments

This research is supported by the U.S. Army Research Office (Grant No. W911NF-12-1-0353), program manager Dr. Asher Rubinstein. The authors also thank Dr. Robert Goldberg (NASA Glenn Research Center) for his valuable feedback.

References

Aboudi, J. (1989). "Micromechanical analysis of composites by the method of cells." *Appl. Mech. Rev.*, 42(7), 193–221.

Bodner, S. R. (2002). *Unified plasticity for engineering applications*, Springer, New York.

Chamis, C. C. (2004). "Probabilistic simulation of multi-scale composite behavior." *Theor. Appl. Fract. Mech.*, 41(1), 51–61.

Eisenberg, M., and Yen, C. (1981). "A theory of multiaxial anisotropic viscoplasticity." *J. Appl. Mech.*, 48(2), 276–284.

Gates, T. S., and Sun, C. (1991). "Elastic/viscoplastic constitutive model for fiber reinforced thermoplastic composites." *AIAA J.*, 29(3), 457–463.

Ghosh, S., Lee, K., and Raghavan, P. (2001). "A multi-level computational model for multi-scale damage analysis in composite and porous materials." *Int. J. Solids Struct.*, 38(14), 2335–2385.

Gilat, A., Goldberg, R. K., and Roberts, G. D. (2002). "Experimental study of strain-rate-dependent behavior of carbon/epoxy composite." *Compos. Sci. Technol.*, 62(10), 1469–1476.

Goldberg, R. K. (2000). "Implementation of laminate theory into strain rate dependent micromechanics analysis of polymer matrix composites." National Aeronautics and Space Administration, Glenn Research Center, Cleveland.

Goldberg, R. K. (2001). "Implementation of fiber substructuring into strain rate dependent micromechanics analysis of polymer matrix composites." National Aeronautics and Space Administration, Glenn Research Center, Cleveland.

Goldberg, R. K., Roberts, G. D., and Gilat, A. (2004). "Analytical studies of the high strain rate tensile response of a polymer matrix composite." *J. Adv. Mater.*, 36(3), 14–24.

Goldberg, R. K., Roberts, G. D., and Gilat, A. (2005). "Implementation of an associative flow rule including hydrostatic stress effects into the high strain rate deformation analysis of polymer matrix composites." *J. Aerosp. Eng.*, 10.1061/(ASCE)0893-1321(2005)18:1(18), 18–27.

Hallquist, J. O. (2007). "LS-DYNA keyword user's manual." Livermore Software Technology Corporation, Livermore, CA.

Hashin, Z. (1980). "Failure criteria for unidirectional fiber composites." *J. Appl. Mech.*, 47(2), 329–334.

Hettich, T., Hund, A., and Ramm, E. (2008). "Modeling of failure in composites by X-FEM and level sets within a multiscale framework." *Comput. Methods Appl. Mech. Eng.*, 197(5), 414–424.

Jenq, S. T., Jing, H. S., and Chung, C. (1994). "Predicting the ballistic limit for plain woven glass/epoxy composite laminate." *Int. J. Impact Eng.*, 15(4), 451–464.

Laurin, F., Carrere, N., and Maire, J. (2007). "A multiscale progressive failure approach for composite laminates based on thermodynamical viscoelastic and damage models." *Compos. Part A: Appl. Sci. Manuf.*, 38(1), 198–209.

Liu, K. (2011). "Micromechanics based multiscale modeling of the inelastic response and failure of complex architecture composites." Doctoral dissertation, Arizona State Univ., Tempe, AZ.

Liu, K. C., Chattopadhyay, A., Bednarcyk, B., and Arnold, S. M. (2011). "Efficient multiscale modeling framework for triaxially braided composites using generalized method of cells." *J. Aerosp. Eng.*, 10.1061/(ASCE)AS.1943-5525.0000009, 162–169.

Liu, K. C., and Ghoshal, A. (2014). "Validity of random microstructures simulation in fiber-reinforced composite materials." *Compos. Part B: Eng.*, 57, 56–70.

Mital, S., Murthy, P., and Chamis, C. (1995). "Micromechanics for ceramic matrix composites via fiber substructuring." *J. Compos. Mater.*, 29(5), 614–633.

Naito, K., Tanaka, Y., Yang, J., and Kagawa, Y. (2008). "Tensile properties of ultrahigh strength PAN-based ultrahigh modulus pitch-based and high ductility pitch-based carbon fibers." *Carbon*, 46(2), 189–195.

Paley, M., and Aboudi, J. (1992). "Micromechanical analysis of composites by the generalized cells model." *Mech. Mater.*, 14(2), 127–139.

Pindera, M., and Bednarcyk, B. A. (1999). "An efficient implementation of the generalized method of cells for unidirectional, multi-phased composites with complex microstructures." *Compos. Part B: Eng.*, 30(1), 87–105.

Pineda, E. J. (2012). "A novel multiscale physics-based progressive damage and failure modeling tool for advanced composite structures." Doctoral dissertation, Univ. of Michigan, Ann Arbor, MI.

Pineda, E. J., Waas, A. M., Bednarcyk, B. A., Collier, C. S., and Yarrington, P. W. (2009). "Progressive damage and failure modeling in notched laminated fiber reinforced composites." *Int. J. Fract.*, 158(2), 125–143.

Robertson, D., and Mall, S. (1993). "Micromechanical relations for fiber-reinforced composites using the free transverse shear approach." *J. Compos. Technol. Res.*, 15(3), 181–192.

Schapery, R. (1990). "A theory of mechanical behavior of elastic media with growing damage and other changes in structure." *J. Mech. Phys. Solids*, 38(2), 215–253.

Schwarz, G. (1978). "Estimating the dimension of a model." *Ann. Stat.*, 6(2), 461–464.

Sicking, D. L. (1992). "Mechanical characterization of nonlinear laminated composites with transverse crack growth." Doctoral dissertation, Univ. Microfilms International, Ann Arbor, MI.

Souza, F., Allen, D., and Kim, Y. (2008). "Multiscale model for predicting damage evolution in composites due to impact loading." *Compos. Sci. Technol.*, 68(13), 2624–2634.

Sun, B., Pan, H., and Gu, B. (2014). "Tensile impact damage behaviors of co-woven-knitted composite materials with a simplified microstructure model." *Text. Res. J.*, 84(16), 1742–1760.

Sun, C., and Chen, J. (1989). "A simple flow rule for characterizing nonlinear behavior of fiber composites." *J. Compos. Mater.*, 23(10), 1009–1020.

Sun, C., and Chen, J. (1991). "A micromechanical model for plastic behavior of fibrous composites." *Compos. Sci. Technol.*, 40(2), 115–129.

Tabiei, A., Yi, W., and Goldberg, R. (2005). "Non-linear strain rate dependent micro-mechanical composite material model for finite element impact and crashworthiness simulation." *Int. J. Non Linear Mech.*, 40(7), 957–970.

Thiruppukuzhi, S. V., and Sun, C. (2001). "Models for the strain-rate-dependent behavior of polymer composites." *Compos. Sci. Technol.*, 61(1), 1–12.

Tsai, J., and Sun, C. (2002). "Constitutive model for high strain rate response of polymeric composites." *Compos. Sci. Technol.*, 62(10), 1289–1297.

Voyiadjis, G. Z., Deliktas, B., and Aifantis, E. C. (2001). "Multiscale analysis of multiple damage mechanisms coupled with inelastic behavior of composite materials." *J. Eng. Mech.*, 10.1061/(ASCE)0733-9399(2001)127:7(636), 636–645.

Weeks, C., and Sun, C. (1998). "Modeling non-linear rate-dependent behavior in fiber-reinforced composites." *Compos. Sci. Technol.*, 58(3), 603–611.

Whitney, J. (1993). "A laminate analogy for micromechanics." *Proc., American Society for Composites*, Technomic Publishing AG, Basel, Switzerland, 785–785.

Yekani Fard, M., Chattopadhyay, A., and Liu, Y. (2012a). "Influence of load type and stress gradient on flexural strength of epoxy resin polymeric material." *J. Aerosp. Eng.*, 10.1061/(ASCE)AS.1943-5525.0000228, 55–63.

Yekani Fard, M., Chattopadhyay, A., and Liu, Y. (2012b). "Multi-linear stress–strain and closed-form moment curvature response of epoxy resin materials." *Int. J. Mech. Sci.*, 57(1), 9–18.

Yekani Fard, M., Liu, Y., and Chattopadhyay, A. (2011a). "Analytical solution for flexural response of epoxy resin materials." *J. Aerosp. Eng.*, 10.1061/(ASCE)AS.1943-5525.0000133, 395–408.

Yekani Fard, M., Liu, Y., and Chattopadhyay, A. (2011b). "Characterization of epoxy resin including strain rate effects using digital image correlation system." *J. Aerosp. Eng.*, 10.1061/(ASCE)AS.1943-5525.0000127, 308–319.

Yen, C. (2002). "Ballistic impact modeling of composite materials." *Proc., 7th Int. LS-DYNA Users Conf.*, Livermore Software Technology Corporation, Livermore, CA, 22060–26218.

Yu, Q., and Fish, J. (2002). "Multiscale asymptotic homogenization for multiphysics problems with multiple spatial and temporal scales: A coupled thermo-viscoelastic example problem." *Int. J. Solids Struct.*, 39(26), 6429–6452.

Zhu, L. (2006). "Multiscale high strain rate models for polymer matrix composites." Doctoral dissertation, Arizona State Univ., Tempe, AZ.

Zhu, L., Chattopadhyay, A., and Goldberg, R. K. (2006a). "A 3D micromechanics model for strain rate dependent inelastic polymer matrix composites." *Proc., 47th AIAA/ASME/ASCE/AHS/ASC Structures, Structural Dynamics and Materials Conf*, American Institute of Aeronautics and Astronautics (AIAA), Reston, VA.

Zhu, L., Chattopadhyay, A., and Goldberg, R. K. (2006b). "Nonlinear transient response of strain rate dependent composite laminated plates using multiscale simulation." *Int. J. Solids Struct.*, 43(9), 2602–2630.

Zhu, L., Chattopadhyay, A., and Goldberg, R. K. (2008). "Failure model for rate-dependent polymer matrix composite laminates under high-velocity impact." *J. Aerosp. Eng.*, 10.1061/(ASCE)0893-1321(2008)21:3(132), 132–139.

Zhu, L., Kim, H. S., Chattopadhyay, A., and Goldberg, R. K. (2005). "Improved transverse shear calculations for rate-dependent analyses of polymer matrix composites." *AIAA J.*, 43(4), 895–905.